ACS Biomaterials SCIENCE & ENGINEERING

Article

pubs.acs.org/journal/abseba

Rational Design and Hierarchical Assembly of a Genetically Engineered Resilin−Silk Copolymer Results in Stiff Hydrogels

Sheng-Chen Huang,[†] Zhi-Gang Qian,[†] Ao-Huan Dan, Xiao Hu, Ming-Liang Zhou, and Xiao-Xia Xia*

State Key Laboratory of Microbial Metabolism, Joint International Research Laboratory of Metabolic & Developmental Sciences, and School of Life Sciences and Biotechnology, Shanghai Jiao Tong University, 800 Dongchuan Road, Shanghai 200240, People's Republic of China

Supporting Information

ABSTRACT: Genetically engineered protein polymers, which can combine different unique peptide sequences from natural protein materials, offer great opportunities for making advanced materials with well-defined structures and properties. Here we report for the first time biosynthesis and self-assembly of a recombinant resilin−silk (RS) copolymer consisting of repeating units of silk and resilin blocks. The copolymer in aqueous solution self-assembled into nanoparticles, and the assembled nanoparticles further form nano- to microscale fibers in a time-dependent manner at body temperature, whereas such fibers were not formed upon incubation of the copolymer at either low or high temperatures. In contrast, a resilin-like polypeptide without the silk blocks exhibited a typical thermoresponsive dual-phase transition behavior and was incapable of self-assembling into fibers. More interestingly, the microscale fibers self-assembled from a moderately concentrated RS solution (20 wt %) could interact to give a self-supporting, semitransparent hydrogel with elastic modulus at approximately 195 Pa. Furthermore, photo-cross-linking of either freshly prepared or annealed RS copolymer led to the formation of stiff hydrogels and the material mechanical property was superior upon annealing of the RS solution for a longer time up to 4 h, with elastic modulus ranging from 2.9 to 7.0 kPa. These results not only shed light on the fundamental hierarchical assembly mechanism of a new family of genetically engineered RS copolymer but also suggest future opportunities for these thermoresponsive polymers in fabrication of hydrogel materials with tunable mechanical properties for diverse applications.

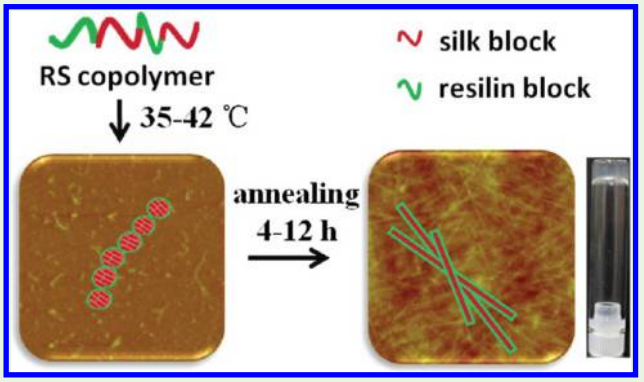

KEYWORDS: *self-assembly, resilin−silk copolymer, genetic engineering, hydrogel, photochemical cross-linking*

INTRODUCTION

Self-assembly is one of the most important mechanisms that nature exploits to create remarkable protein materials, such as silk, resilin, collagen, and elastin. These materials are mainly composed of polypeptide sequences with defined structures, such as α-helixes, β-sheets, coiled-coils, β-turns, and β-spirals.[1−3] Inspired by nature, many research groups are focusing on the design and biosynthesis of artificial protein polymers by employing the above unique peptide sequences as consensus motifs, and by controlling their self-assembly processes to fabricate designer materials.[4−11] Each of the individual peptide sequences endowing diverse chemical, physical or biological properties can be recombined at the DNA level for the synthesis of multiblock protein copolymers.[6,7] These developments highlight the exciting opportunities for the genetically engineered protein polymers as novel materials for tissue engineering, drug delivery, sensors, and many other applications.[12−16]

Among a variety of natural elastic materials, resilin has been well-recognized for its remarkable properties characterized by low stiffness, high extensibility, and exceptional resilience.[17,18] The extraordinary material is normally found in specialized regions of the cuticle of most insects. The pioneering study by Ardell and Anderson identified the gene sequence (CG15920) encoding pro-resilin from the fruitfly *Drosophila melanogaster*, which opened routes to recombinant biosynthesis of resilin-like polypeptides with properties comparable to those of native resilin. The first recombinant resilin-like protein, rec1-resilin was derived from the first exon of the *Drosophila* CG15920 gene comprising 17 copies of the elastic repeat motif, GGRPSDSYGAPGGGN.[19] Rec1-resilin, which was expressed as a soluble protein in *Escherichia coli*, could be photo-cross-linked into a rubberlike biomaterial with resilience comparable to that of natural resilin, even though this recombinant protein contained only Exon I region of the natural pro-resilin.[20] Following the synthesis of rec1-resilin, other resilin-like proteins have also been generated that contained different repetitive consensus motifs derived from different insect

Received: June 4, 2017
Accepted: June 13, 2017
Published: June 13, 2017

DOI: 10.1021/acsbiomaterials.7b00353
ACS Biomater. Sci. Eng. 2017, 3, 1576−1585

sources.[21,22] Further spectroscopic investigations indicated that these resilin-like proteins are largely disordered with no apparent or little α-helical and β-sheet secondary structures.[23,24] More interestingly, rec1-resilin was found to display multiple-stimuli responsiveness to several factors such as temperature, pH, and light, which has scarcely been offered and reported for either synthetic or natural biopolymers.[25,26] In particular, rec1-resilin exhibited dual-phase transition behavior (DPB) with a lower critical solution temperature (UCST) at ~6 °C and an upper critical solution temperature (LCST) at ~70 °C. As a result, rec1-resilin was soluble with a hydrodynamic diameter of ~11 nm at temperatures between its UCST and LCST, whereas the protein self-organized and underwent phase separation below and above those temperatures.[25] These unique molecular flexibility, self-organization, and physical attributes of resilin indicate the great potential of resilin consensus motifs for the development of novel intelligent materials.[26−28]

Indeed, investigations have been motivated toward the design of chimeric protein materials that combine the unique properties of resilin and other structural motifs. For example, a chimeric resilin−elastin−collagen (REC) polypeptide was designed and recombinantly produced, which exhibited a high propensity to self-assemble into fibers with a Young's modulus between 0.1 and 3 MPa. Notably, the REC fibers were orders of magnitude softer than collagen-like bundles, most likely due to the introduction of the softer resilin and elastin domains.[29] In another interesting example, a multiblock protein was designed, in which folded GB1 domains from the streptococcal B1 immunoglobulin-binding domain of protein G were interspersed with random-coil resilin-based sequences. The multiblock design combined the unique mechanical properties of each element and yielded a rubber-like biomaterial with a measured Young's modulus (50−70 kPa) that was similar to that of myofibrils (60−100 kPa). Moreover, this biomaterial showed high resilience at low strain but exhibited shock-absorber-like properties at high strain, comparable to the passive elastic characteristics of muscles.[30] In addition to the structural motifs, biologically functional domains can also be combined into recombinant resilin-like polypeptides to impart cell adhesion (RGDSP), proteolytic degradation (GPQGIWGQ), and/or heparin immobilization (KAAKRP-KAAKDKQTK).[17] The above studies suggest an encouraging strategy to the development of genetically engineered resilin-based materials with tailored mechanical properties and biological functionalities for a variety of biomedical applications.

We are also interested in the exploration of the unique elastomeric resilin for design and biosynthesis of genetically engineered block copolymers. Because of the intrinsically disordered feature, resilin lacks the mechanical strength and stiffness range required for most tissue engineering applications.[31] To overcome this obstacle, a recent study by the Choudhury group mixed recombinant rec1-resilin with regenerated silk fibroin for photo-cross-linking, which resulted in hydrogels with enhanced storage modulus, although the material properties and reproducibility were still less controlled due to the complicated compositions of the regenerated silk fibroin.[32] Therefore, we propose the design and biosynthesis of genetically engineered resilin-silk (RS) copolymers consisted of repeating units of silk-like and resilin-like blocks. The silk-like (GAGAGS) blocks have been reported to spontaneously assemble into a β-sheet structure, which is characterized by its stability and responsible for the high tensile strength of silk fibroin,[33−37] whereas the resilin-like (GGRPSDSYGAPGGGN) blocks are highly hydrated and responsive to temperature with a unique dual-phase transition behavior.[26] Because of the dissimilar polarity between the silk and resilin blocks, RS copolymers are hypothesized to self-assemble into micelles and other higher ordered structures resulting in biomaterials with improved stiffness. Furthermore, we hypothesize that the self-assembly of RS copolymers could be manipulated based on the thermoresponsive property of resilin blocks, thus offering a second level of modulation over the biomaterial property.

Herein, we report the design and biosynthesis of a genetically engineered RS copolymer for the first time. The self-assembly of the copolymer will be explored at diverse temperatures over a time period of 12 h. A recombinant resilin-like polypeptide without the silk blocks was also synthesized and included as a control for comparison. Next, the self-assembled RS copolymer was either physically or photochemically cross-linked to form hydrogels, which exhibited interesting preassembly dependent rheological properties.

MATERIALS AND METHODS

Chemicals and Materials. Ampicillin, imidazole and isopropyl-β-D-thiogalactopyranoside (IPTG) were purchased from Sangon Biotech (Shanghai, China). Ni-NTA agarose (Catalog No. 30230) and tris(2,2′-bipyridyl)dichlororuthenium(II) hexahydrate (Catalog No. 224758) were obtained from Qiagen (Hilden, Germany) and Sigma (St. Louis, MO), respectively. Yeast extract and tryptone were purchased from Oxoid (Basingstoke, Hampshire, U.K.). Chemically competent cells of *E. coli* DH5α, TOP10 and BL21(DE3), TIANprep Mini Plasmid Kit, and TIANgel Midi Purification Kit were purchased from TIANGEN Biotech (Beijing, China). PrimeSTAR Max DNA polymerase for polymerase chain reaction (PCR) was obtained from Takara Biotechnology Co., Ltd. (Dalian, China). Restriction endonucleases, calf intestinal alkaline phosphatase (CIP), and T4 DNA ligase were obtained from New England Biolabs (Ipswich, MA). Amicon Ultra-15 centrifugal filter units with Ultracel-3K membranes, and dialysis tubing (3.5 kDa molecular weight cutoff) were obtained from Millipore (Billerica, MA) and Spectrum Laboratories (Phoenix, AZ), respectively. The Pierce BCA Protein Assay kit for protein quantification was purchased from Thermo Scientific (Product No. 23225; Rockford, IL).

Construction of Expression Plasmids. A tailor-made vector pET-19b3, previously developed for recombinant expression of silk-elastin-like protein polymers,[34] was employed to construct expression plasmids encoding resilin-silk protein polymers in this study. First, a deoxyribonucleic acid (DNA) sequence encoding the resilin-silk sequence R4S4 [$(GGRPSDSYGAPGGGN)_4(GAGAGS)_4$] was purchased as a synthetic gene that was cloned into the *Sfi*I site of plasmid pMA-RQ from Invitrogen (Shanghai, China). The monomer DNA sequence was then liberated by digesting plasmid pMA-RQ-R4S4 with restriction enzyme *Ban*II, isolated by agarose gel electrophoresis, and purified using the TIANgel Purification Kit. The purified monomer DNA was then self-ligated with T4 DNA ligase at 16 °C for 12 h to yield DNA multimers. Next, the *Ban*II- and CIP-treated pET-19b3 plasmid was added to the reaction mixture and incubated for an additional 12 h. The ligation mixture was used to transform chemically competent cells of *E. coli* DH5α. The resulting transformants harbored recombinant plasmids that carried the repetitive R4S4 genes of varying lengths. These expression plasmids were identified by double digest with *Nde*I and *Bam*HI-HF and further confirmed by sequencing with forward T7 primer (5′-TAATACGACTCACTATAGGG-3′) and reverse T7-Term primer (5′-GCTAGTTATTGCTCAGCGG-3′). Plasmid pR4S4−5 was thus obtained that encoded 5 repeats of R4S4 under transcriptional control of the strong T7 promoter.

The DNA sequence encoding four repeats of resilin-like sequence (GGRPSDSYGAPGGGN) was PCR-amplified from plasmid pMA-

DOI: 10.1021/acsbiomaterials.7b00353
ACS Biomater. Sci. Eng. 2017, 3, 1576−1585

RQ-R4S4 with PrimeSTAR Max DNA polymerase and primers Fr4NdeNhe (5′-AATCATATGGCTAGCGGCGGTCGTCCTTCA-GATAGT-3′) and Rr4XhoSpe (5′-AATCTCGAGACTAGTGTTGC-CACCACCTGGTGCA-3′). The PCR product was double digested with *Nde*I and *Xho*I, and ligated with the 5.7-kb, *Nde*I-*Xho*I fragment of the expression vector pET-19b (Novagen, Madison, WI). The ligation mixture was subsequently transformed into chemically competent cells of *E. coli* DH5α. The target recombinant plasmid pET19b-R4 was identified by double digest with *Nde*I and *Eco*RI-HF and further confirmed by sequencing. To express 8 repeats of the resilin-like sequence, plasmid pET19b-R8 was constructed by ligating the 1.1-kb, *Pvu*I-*Nhe*I fragment of pET19b-R4 to the 5.0-kb, *Spe*I-*Pvu*I fragment of pET19b-R4, followed by transformation into *E. coli* TOP10. Likewise, plasmid pET19b-R16 was constructed by ligating the 1.3-kb, *Pvu*I-*Nhe*I fragment of pET19b-R8 to the 5.1-kb, *Spe*I-*Pvu*I fragment of pET19b-R8. Finally, the 1.7-kb, *Pvu*I-*Nhe*I fragment of pET19b-R16 was ligated with the 5.5-kb, *Spe*I-*Pvu*I fragment of pET19b-R16 to make plasmid pET19b-R32, which allowed expression of 32 repeats of the resilin-like sequence under the strong T7 promoter.

Protein Expression, Purification, and Identification. Chemically competent cells of *E. coli* BL21(DE3) were transformed with either plasmid pR4S4-5 or pET19b-R32, and incubated overnight on Luria−Bertani (LB) solid medium with 50 μg mL^{-1} of ampicillin. A single colony of each recombinant strain was inoculated into selective LB liquid medium in a test tube and incubated for about 12 h at 37 °C and 220 rpm in a rotary shaker. The overnight culture was then diluted into 100 mL of fresh LB in a shake flask and incubated until the cell optical density at 600 nm (OD_{600}) reached ∼3−4. This seed culture was inoculated into 800 mL of selective Terrific broth (per liter: 12.54 g of K_2HPO_4, 2.31 g of KH_2PO_4, 24 g of yeast extract, 12 g of tryptone, 5 g of glycerol) in a 2 L baffled flask. These cultures were incubated for ∼6 h and then induced with 1 mM IPTG at 16 °C for 12−14 h. The induced cells were harvested by centrifugation, resuspended in 20 mM Tris-HCl buffer (pH 8.0), and then lysed using a high pressure homogenizer. Following centrifugation, the supernatant was loaded onto a Ni-NTA agarose column for affinity purification. Upon elution from the column, the target proteins were extensively dialyzed against water, concentrated using a centrifugal filter unit and freeze-dried. The purity of the proteins was analyzed via 10% SDS-PAGE with Coomassie staining. The molecular weights of the purified proteins were confirmed by matrix-assisted laser desorption ionization time-of-flight (MALDI-TOF) mass spectrometry at Shanghai Applied Protein Technology Co. Ltd. (Shanghai, China).

Size Analysis by Dynamic Light Scattering (DLS). Each lyophilized protein polymer was dissolved in deionized water at a final concentration of 10 mg mL^{-1}. The freshly prepared protein solutions were then transferred into precooled cuvettes at 4 °C and directly used for DLS analysis at increasing temperatures from 4 to 70 °C. The samples were equilibrated at the indicated temperature for 10 min before DLS measurement using a Zetasizer Nano S system equipped with a temperature controller (Malvern Instruments, Worcestershire, U.K.). Alternatively, the fresh protein solutions were incubated at 37 °C for annealing over a time period of 12 h. The annealed samples were then subjected to particle size distribution analysis using the above DLS system. The size distribution data were collected from three biological replicates and analyzed using the Zetasizer version 7.04 software (Malvern Instruments).

Atomic Force Microscopy (AFM). Two types of protein samples were analyzed by AFM in tapping mode using a multimode AFM (Bruker, Germany) with a Nanoscope IIIa scanning probe controller (Digital Instruments, Santa Barbara, CA). For freshly prepared samples, 10 μL of each protein in deionized water at a low concentration of 0.1 μg mL^{-1} was casted on mica surfaces and allowed to dry at the indicated temperatures for ∼12 h. Alternatively, freshly prepared protein solutions at 10 mg mL^{-1} were incubated at either 4, 37, or 70 °C for 4−12 h. Photographs of the aged protein solutions were taken after loading each sample into a Suprasil quartz cuvette (10 mm lightpath; Hellma, Müllheim, Germany) using an EOS 700D camera (Canon, Tokyo, Japan). Similarly, 10 μL of each aged protein solution was casted on mica surfaces and allowed to dry at the respective preincubation temperatures for ∼12 h. In all AFM experiments, a commercial silicon tip probe was used, which had a spring constant of ∼3 N m^{-1}, and the scan rate was 2 Hz. The AFM images were collected with a scanning window of 2 μm and further processed with the Nanoscope analysis v5.30 software (Bruker).

Preparation of Hydrogels. Two types of hydrogels, self-annealed and photochemically cross-linked, were prepared from each of the protein polymers. To prepare self-annealed hydrogels, we dissolved a lyophilized protein in deionized water at a final concentration of 200 mg mL^{-1} and then transferred it into glass tubes. The tubes were promptly incubated at 37 °C in a water bath, taken out at an interval of 4 h, and inversed to evaluate the formation of self-supporting hydrogels by taking photographs with the Canon EOS 700D camera (Canon). To prepare hydrogels by photochemical cross-linking, we mixed each protein solution, either freshly prepared or aged for 2−4 h, with $[Ru(bpy)_3]^{2+}$ and ammonium persulfate and irradiated in glass tubes for 20−30 s at 10 cm away from the sample with a 200-W white light source. The final concentrations of the protein, $[Ru(bpy)_3]^{2+}$, and ammonium persulfate in the mixture were 200 mg mL^{-1}, 2 mM, and 10 mM, respectively.

Rheological Measurements. Rheological characterization of the hydrogels was conducted on a stress-controlled AR-G2 rheometer with a 40 mm parallel-plate configuration (TA Instruments, New Castle, DE). In one setup, a freshly prepared protein solution (500 μL) at a concentration of 200 mg mL^{-1} was loaded onto the prewarmed bottom plate at 37 °C. Then the top plate was lowered to a gap distance of 310 μm, with hydrogenated silicone added around the circumference to minimize dehydration. Subsequently, a time sweep was carried out at 37 °C with a strain of 1% and a frequency of 1 Hz. In another setup, freshly prepared protein solution was first incubated at 37 °C for 0−4 h before mixing with the photochemical cross-linking reagents. Then the mixture (500 μL) with 2 mM $[Ru(bpy)_3]^{2+}$, 10 mM ammonium persulfate, and protein at a final concentration of 200 mg mL^{-1} was transferred onto the prewarmed bottom plate at 37 °C and incubated for additional 5 min. Upon irradiation with white light for photochemical cross-linking as described above, frequency sweeps were performed for the resulting hydrogels with a constant strain of 1% and logarithmic ramping from 0.1 to 100 rad s^{-1}.

Scanning Electron Microscopy (SEM). Hydrogels were first lyophilized and the specimens were then coated with gold using a Leica EM SCD050 sputtering device with a water-cooled sputter head (Leica Microsystems GmbH, Vienna, Austria). SEM analyses were then performed using a model S-3400N scanning electron microscope (Hitachi, Tokyo, Japan).

Structural Characterization by Fourier Transform Infrared Spectroscopy (FTIR). FTIR spectra were acquired in transmission mode at room temperature by using a Nicolet 6700 spectrometer (Thermo Fisher Scientific Inc., Madison, WI) combined with a deuterated triglycine sulfate detector. Prior to analyses, hydrogels were freeze-dried for 3 days in order to fully dehydrate the samples using the Labconco FreeZone Plus 6 lyophilizer. For each sample, 64 scans were coadded at wave numbers ranging from 400 to 4000 cm^{-1} with a resolution of 4 cm^{-1}. The background spectra were also taken under the same conditions and subtracted from each sample scan. The infrared spectra in the range of 1600−1700 cm^{-1} (Amide I region) were analyzed using the OMNIC software (Thermo Fisher Scientific).

Cyto-compatibility. The photochemically cross-linked RS hydrogels was subjected to cyto-compatibility assessments in vitro. Water solutions of RS, either freshly prepared or aged at 37 °C for either 2 or 4 h, were mixed with the photochemical reagents in wells of a flat bottom 96-well cell culture plate (Nest Biotechnology Co., Ltd., Wuxi, China). The mixtures with RS, $[Ru(bpy)_3]^{2+}$ and ammonium persulfate at final concentrations of 200 mg mL^{-1}, 2 mM, and 10 mM, respectively, were irradiated with the white light source as described above. The resulting hydrogels were soaked and washed in sterile phosphate buffered saline (PBS) for 24 h, with change of fresh buffer every 6 h. The mouse preosteoblast cell line tested (MC3T3-E1) was obtained from Cell Bank of the Chinese Academy of Sciences

DOI: 10.1021/acsbiomaterials.7b00353
ACS Biomater. Sci. Eng. 2017, 3, 1576−1585

(Shanghai, China) and cultured as described in our recent study.[16] The cells from a seed culture were evenly inoculated onto the hydrogels and a tissue culture plate (TCP) at a density of 5×10^3 cells/well. Cell viability was examined at 48 h postseeding by using the LIVE/DEAD Viability/Cytotoxicity Kit (Invitrogen).

RESULTS AND DISCUSSION

Design and Biosynthesis of RS and R32. To test our hypothesis, a genetically engineered RS copolymer was designed with each monomer repeat consisting of silk-like (GAGAGS) peptide blocks produced by silkworm *Bombyx mori* and resilin-like (GGRPSDSYGAPGGGN) blocks from the first exon of the fruitfly *D. melanogaster* CG15920 gene. DNA encoding the monomer repeat was chemically synthesized and the monomer DNA was multimerized through the concatemerization strategy employing endonuclease restriction site *Ban*II (5′-GGGCTC-3′). The multimer gene was then cloned into plasmid pET-19b3, a tailor-made vector for the cloning of silk-elastin-like protein polymers in our previous studies.[34] This allowed seamless cloning without the introduction of extra amino acids at the junctions between monomers. An expression plasmid was thus generated that encoded 5 repeats of $(GGRPSDSYGAPGGGN)_4(GAGAGS)_4$, which was hereafter termed as RS (Figure 1A). In addition, another expression

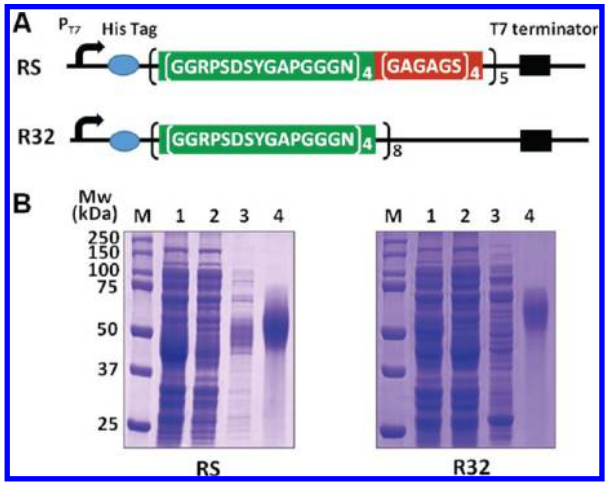

Figure 1. (A) Genetic constructs of recombinant RS and R32. (B) Coomassie-stained 10% SDS-PAGE gel analysis of biosynthesized RS and R32 from recombinant *E. coli* BL21(DE3). Lane 1, whole cell lysate; Lane 2, flow-through from Ni-NTA agarose column; Lane 3, washing fraction; Lane 4, eluted fraction.

plasmid encoding 32 resilin-like (GGRPSDSYGAPGGGN) blocks was also constructed as explicitly described in the Method section. This resilin-like polypeptide, termed as R32, was included as a control in this study.

The two protein polymers were recombinantly expressed in the bacterial host *E. coli* BL21 (DE3) and purified using immobilized-metal-affinity chromatography. Upon elution from the Ni-NTA agarose column, the purified protein polymers showed at least 90% purity, as confirmed by SDS-PAGE analysis (Figure 1B). Although RS and R32 migrated as smearing bands with apparent molecular weights at approximately 50−60 kDa on the SDS-PAGE gels, the two proteins were verified by matrix-assisted laser desorption ionization time-of-flight (MALDI-TOF) mass spectrometry. As revealed by the mass spectrometric analysis, the two recombinant proteins had molecular weights at 37.8 and 49.2 kDa, respectively, which were consistent with the expected theoretical values (Figure S1). The yields of the purified protein polymers were in the range of 50−100 mg L^{-1} of bacterial culture in shake flasks.

Thermal Responsive Assembly of RS. It has been demonstrated that recombinant resilin-like polypeptide is thermoresponsive and exhibits dual-phase transition behavior.[25] To examine whether the incorporation of silk blocks would affect this thermoresponsive behavior, we conducted dynamic light scattering (DLS) analysis to monitor the hydrodynamic diameter (Dh) of RS and R32 in solutions (Figure S2). As expected, R32 exhibited a typical dual phase transition behavior with a UCST and a LCST at ∼4 °C and ∼60 °C, respectively. However, such dual phase transitions were not observed for RS, and the incorporation of silk blocks complicated the effects of temperature on the Dh of the copolymer. In general, the size of RS particles increased from ∼369 nm at 4 °C to 1149 nm at 70 °C. Interestingly, at temperatures between 25 and 45 °C, RS was found to form two populations of nanostructures with differing sizes. This prompted us to further examine the formed nanostructures in details.

Atomic force microscopy (AFM) was performed to study the self-assembled nanostructures of RS and R32 at diverse temperatures (Figure 2). RS formed uniform spherical particles with a diameter of 10−20 nm at 4 °C, and such nanoparticles were also observed at 25 °C, with the coexistence of larger particles of 30−50 nm. Interestingly, two types of nanostructures, nanoparticles with a diameter of 10−20 nm and nanofibrils with a length of 80−200 nm were observed at 37 °C, and these nanofibrils disappeared at 70 °C with the presence of larger nanostrucrures of 70−100 nm, which might arise from the coalescence of the smaller micellar-like particles or the nanofibrils. In contrast, R32 existed as larger nanoparticles at 4 and 70 °C than at the intermediate temperatures, which agreed well with its dual thermal phase transition. Taken together, the AFM and DLS results indicated that RS maintained the thermoresponsive property of resilin, and the incorporation of silk blocks endowed the copolymer an ability to self-assemble into nanofibrils. It appeared that self-assembly of the RS copolymer into nanofibrils was a concerted outcome of both the silk and resilin blocks. At an appropriate range of temperatures where the interaction of silk blocks was stronger than that of resilin blocks, nanofibrils due to the stacking of β-sheets were formed. Indeed, the nanofibrilar structure was observed in the aqueous solution of RS at physiologically relevant temperatures ranging from 35 to 42 °C (Figure S3). However, at temperatures outside this range, the interaction of resilin blocks played a major role in directing the self-assembly of the copolymer, which might mask the propensity of the silk blocks to form nanofibrils. Nonetheless, the detailed mechanisms and molecular events during this temperature-dependent self-assembly of the RS copolymer are still unclear and deserve further investigations.

Time-Dependent Hierarchical Assembly of RS into Nanofibers. As reported previously, the β-sheet forming silk blocks are prone to self-assemble into higher ordered nanofibers.[33,34] To study whether the RS nanofibrils formed at 37 °C could initiate its hierarchical assembly into nanofibers, DLS analysis was first performed to study possible changes in size of the nanostructures at 37 °C (Figure S4). As a control, the R32 nanoparticles were appreciably stable without obvious changes in particle size during a prolonged time period of 12 h. In contrast, RS exhibited a clear evolution in size of the

DOI: 10.1021/acsbiomaterials.7b00353
ACS Biomater. Sci. Eng. 2017, 3, 1576−1585

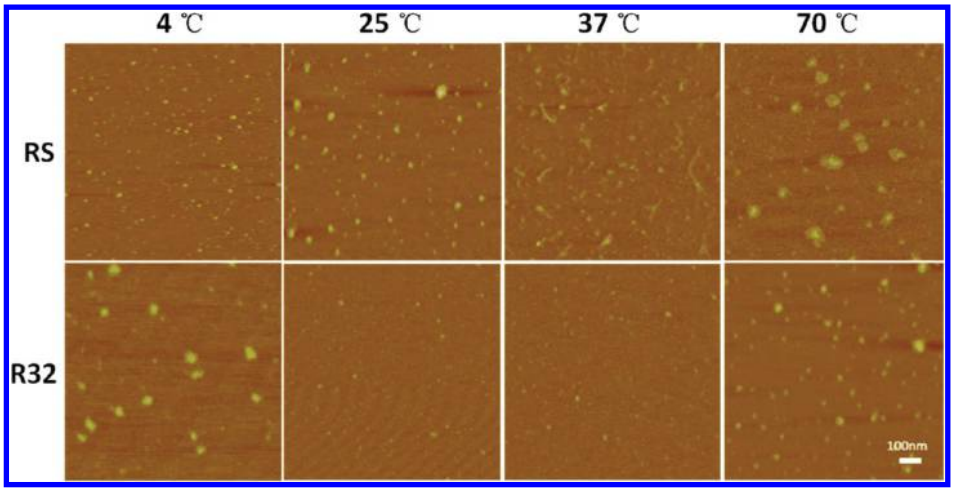

Figure 2. Representative AFM images of the nanostructures for RS and R32 at diverse temperatures. Freshly prepared solution (10 μL) of each protein in deionized water at a concentration of 0.1 μg mL^{-1} was casted on mica surfaces and allowed to dry at the indicated temperatures before AFM analysis.

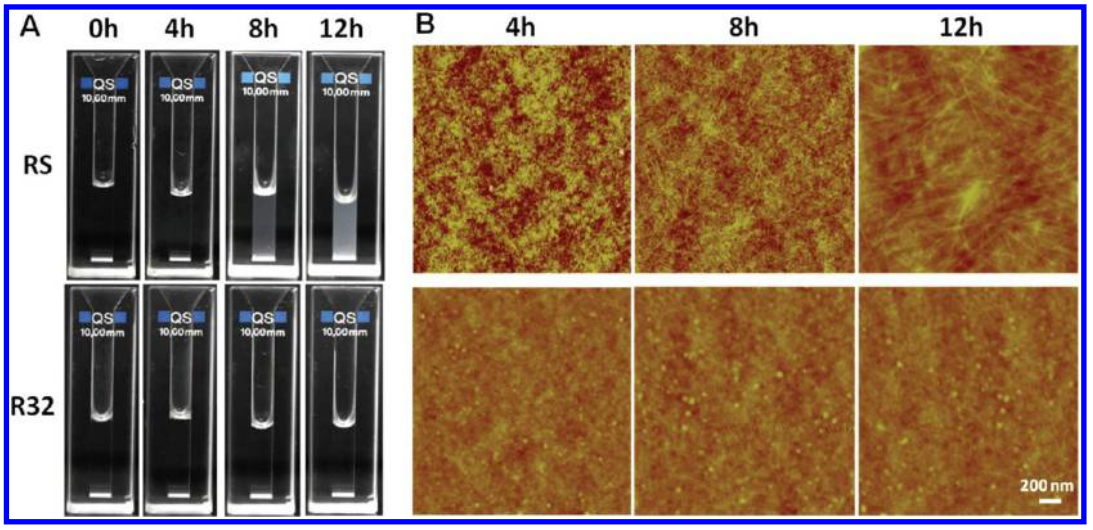

Figure 3. (A) Photographs and (B) AFM images of the nanostructures of protein solutions at a concentration of 10 mg mL^{-1} upon incubation at 37 °C for 4−12 h. Each protein sample was casted on mica surfaces and allowed to dry at 37 °C before AFM analysis.

nanostructures, and microscale structures were even detected at the late stage of incubation. This dramatic increase in sizes of the RS nano- to microscale structures agreed well with turbidity test of the polymer solutions (Figure 3A). Not surprisingly, solution of the RS copolymer turned from transparent to turbid at 8 h, whereas the solution of R32 remained transparent for at least 12 h.

Next, we performed AFM to monitor the morphological changes of RS and R32 upon incubation at 37 °C for 12 h (Figure 3B). It was again confirmed that the morphology and size of R32 nanoparticles were not significantly changed during the time period tested, which was in good agreement with the DLS analysis. However, RS showed a time-dependent growth of the nanofiber structures upon incubation at 37 °C. It was observed that RS assembled into relatively short, curly nanofibers at 4 h, and the curly nanofibers evolved into longer and extended nanofibers at 8 h. Finally, uniform microfibers with a length of ∼1 μm were observed at 12 h. These results demonstrated that RS had undergone hierarchical self-assembly from nanoparticles to curly nanofibrils, and finally into microscale fibers by annealing at 37 °C for about 8−12 h.

Furthermore, we tested whether RS would assemble into nano- to microfibers upon incubation at 4 and 70 °C. As shown in Figure 4A, the RS solution was transparent for at least 12 h at 4 °C, and no significant morphological changes were observed according to the AFM analysis. However, solution of R32 was turbid from beginning of the incubation test at 4 °C, and an increasing amount of large coacervates was formed as revealed by AFM analysis. This observation was as expected, which coincided well with the UCST transition behavior of resilin-like polypeptide. When RS and R32 were incubated at 70 °C, solutions of the two protein polymers became turbid after 4 h incubation (Figure 4B). AFM analysis revealed that many unordered aggregates were formed in the RS solution, whereas R32 mostly existed in the form of small particles and coacervates. These results indicated that neither RS nor R32 self-assembled into nanofibers at 4 and 70 °C, which was possibly due to the strong interaction of resilin blocks at these temperatures that prevented stacking of silk β-sheets into nanofibers.

Formation of Nanofibrous Hydrogel by Physical Cross-linking. Having demonstrated that the RS copolymer

DOI: 10.1021/acsbiomaterials.7b00353
ACS Biomater. Sci. Eng. 2017, 3, 1576−1585

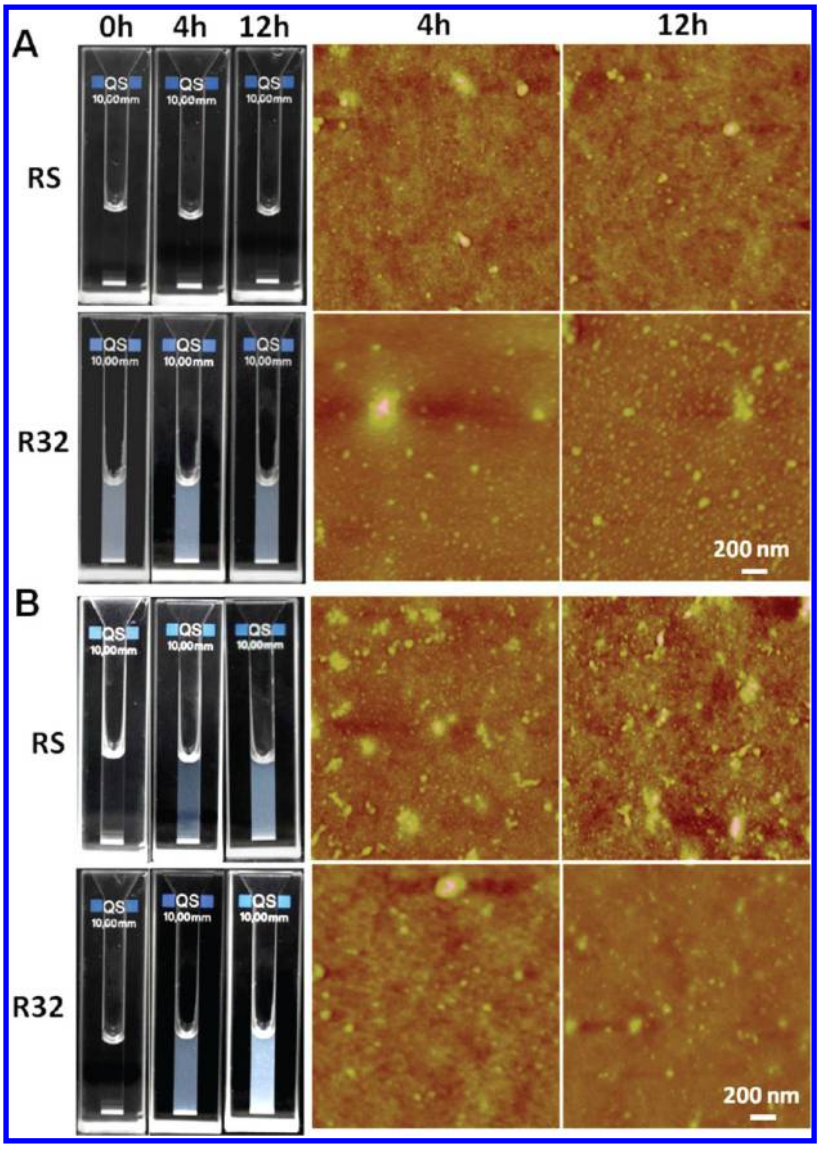

Figure 4. Photographs and AFM images of the nanostructures of protein solutions at 10 mg mL^{-1} upon annealing at (A) 4 and (B) 70 °C for 4−12 h. Each protein was casted on mica surfaces and allowed to dry at the respective preincubation temperatures before AFM analysis.

could self-assemble into nano- to microscale fibers, we next explored whether the assembled structures would enable the formation of hydrogel biomaterials. To test this, freshly prepared solutions of RS and R32 in deionized water at a final protein concentration of 20% (w/v) were incubated at 37 °C in glass tubes, and the tubes were then inverted to evaluate the formation of a self-supporting hydrogel. As shown in Figure 5A, the RS solution became highly viscous upon incubation for 4 h, and turned into a self-supporting, semitransparent hydrogel upon incubation for 8−12 h. The RS hydrogel was found to become opaque and more rigid upon incubation at 37 °C for a longer time (data not shown). In contrast, R32 remained in a liquid state even after 12 h incubation (Figure 5B). Notably, the freshly prepared solutions of 20% (w/v) RS and R32 were also incubated at 4 and 70 °C for 12 h, and no self-supporting hydrogels were formed (data not shown). These results indicated that the self-assembly of RS into nanofibers at 37 °C (Figure 3) was vital for the formation of physically crossed hydrogel network.

To further confirm and quantify the RS hydrogel mechanical behavior, we recorded storage (G') and loss (G'') moduli as a

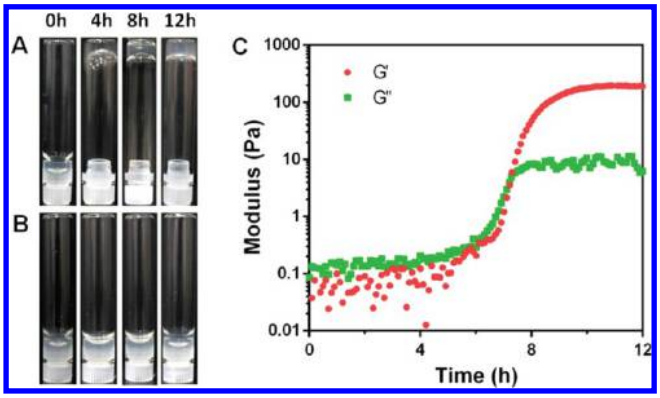

Figure 5. Test of formation of hydrogels by (A) RS and (B) R32. Vials containing freshly prepared solutions of each protein at 20% (w/v) were incubated at 37 °C for 0−12 h. (C) Oscillatory rheological profiles for the freshly prepared RS solution at 20% (w/v). Time sweep in which elastic modulus (G') and loss modulus (G'') are shown as a function of time was performed at 37 °C with a strain of 1% and a frequency of 1 Hz.

DOI: 10.1021/acsbiomaterials.7b00353
ACS Biomater. Sci. Eng. 2017, 3, 1576−1585

function of time at 37 °C using oscillatory rheology (Figure 5C). During the initial 7 h, the value of G' was lower than G'', indicating the solution state of RS. After that, G' increased gradually and reached a plateau value of ∼195 Pa at 10 h, confirming the formation of a soft hydrogel.

To observe the microstructures of the RS hydrogels, we performed scanning electron microscopy (SEM) on the lyophilized hydrogels formed from 20% (w/v) RS solution upon incubation at 37 °C. As shown in Figure 6, the viscous

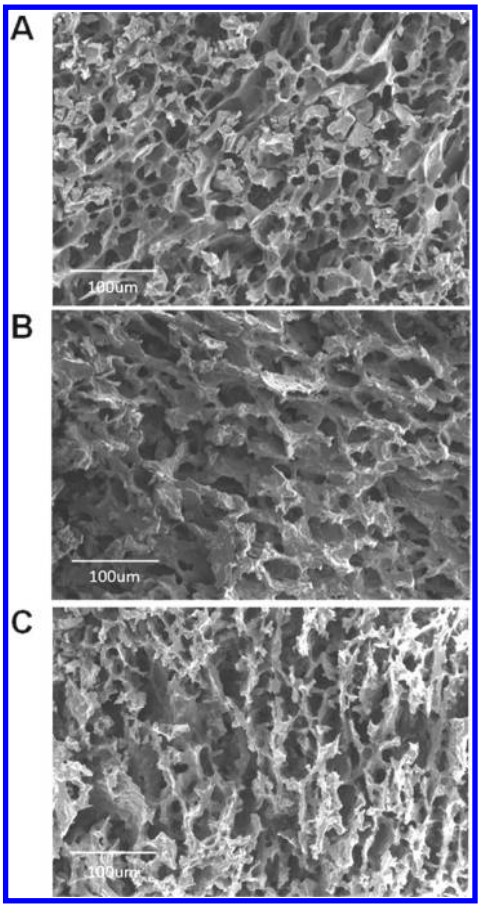

Figure 6. Scanning electron microscopy (SEM) of lyophilized hydrogels formed from 20% (w/v) RS solution upon incubation at 37 °C for (A) 4, (B) 8, and (C) 12 h.

fluid sample with 4 h incubation showed loose, porouslike structures, possibly due to the existence of different, inhomogeneous nanoelements (particles and fibrils), whereas the hydrogels formed upon incubation for 8 and 12 h showed more ordered microstructures that were mainly composed of microfibrils. Notably, the more ordered hydrogel microstructures coincided well with the higher mechanical strength as observed from the oscillatory rheological analysis. In addition, entanglement and physical cross-linking of sheetlike microstructures were observed for the hydrogels, which might be due to the existence of the preassembled nanofibers in the RS copolymer.

Because physiologically relevant systems encounter salts, we also examined whether the physically cross-linked hydrogels could be formed from RS solutions containing saline. To this end, we dissolved lyophilized RS in phosphate-buffered saline (PBS) and incubated at the body temperature (Figure S5). As expected, gelation also occurred upon incubation at a time scale of hours, which was essentially the same as gelation in the deionized water solutions (Figure 5A). These results suggest a facile strategy for the fabrication of physically cross-linked hydrogels by incubating aqueous solutions of RS at the body temperature. On the other hand, the multihour assembly of RS into hydrogels was relatively slow, which might limit its use as an injectable biomaterial for in vivo applications. Further exploration of the physiochemical factors that favor the interaction between the silk blocks may be necessary to achieve faster hierarchical assembly and physically cross-linked biomaterials.

Photo-cross-linking of Preassembled RS Resulted in Stiffer Hydrogels. Previously, an efficient and rapid $[Ru(bpy)^3]^{2+}$-mediated photochemical cross-linking was used to form dityrosine cross-links between the tyrosine residues in rec1-resilin, resulting in a rubberlike biomaterial.[20] This photochemical cross-linking reaction has also been demonstrated for the fabrication of fibrinogen- and gelatin-based tissue sealants,[38,39] mussel protein-based surgical protein glue,[40] and fibrin-based engineered tissue[41] with good biocompatibility. Notably, our RS copolymer contained one tyrosine residue in each resilin motif (GGRPSDSYGAPGGGN), which provided a photochemical cross-linking point between different RS molecules. Therefore, the photochemical method was also employed in this study, with an attempt to explore whether the preassembly of RS into nanofibrils was beneficial for creating stiffer hydrogels. To this end, aqueous solutions of 20% (w/v) RS with and without preincubation at 37 °C were photochemically cross-linked using tris(2,2′-bipyridyl)-dichlororuthenium(II) as the catalyst and ammonium peroxodisulfate as the electron acceptor. It should be noted that the RS solutions were preassembled for no longer than 4 h before the photochemical reactions, because longer incubation at a time of 4−12 h led to the formation of physically cross-linked, solid hydrogels (Figure 5A), which prevented the mixing of the photochemical reaction regents for dityrosine cross-linking.

Following photochemical cross-linking, the linear rheological properties of the equilibrated hydrogels were measured (Figure 7A). Interestingly, an increase in the preincubation time resulted in stiffer hydrogel. For example, 4 h preincubation of the RS copolymer and photochemical cross-linking led to a hydrogel with material stiffness (G') at ∼7000 Pa, which was 2.4-fold higher than that of the photochemically cross-linked hydrogel (2.9 kPa) without preincubation of the RS solution. This result suggested that RS self-assembly in combination with chemical cross-linking provided a useful strategy to increase the stiffness of fabricated hydrogel materials.

Fourier transform infrared spectroscopy (FTIR) analysis was further performed to characterize the conformational structures of the cross-linked hydrogels (Figure S6). Basically, the region from 1600 to 1640 cm^{-1} of FTIR spectra is recognized to be related to the intermolecular and intramolecular β-sheet bands, whereas the region between 1640 and 1660 cm^{-1} is associated with random coils and α-helices.[33,35,42] As shown in Figure 7B, the photochemically cross-linked hydrogels with 2- and 4 h preincubation of the RS solutions showed signals at 1636 and 1627 cm^{-1}, respectively, which indicated the formation of β-sheet structures, whereas the lack of preincubation led to a hydrogel without obvious β-sheet structures as its FTIR spectra peak was at 1642 cm^{-1}. The above results indicated that preincubation of the RS solution induced the formation of silk crystallization, which might explain why the resulting hydrogels showed higher material stiffness than that without preassembly.

DOI: 10.1021/acsbiomaterials.7b00353
ACS Biomater. Sci. Eng. 2017, 3, 1576−1585

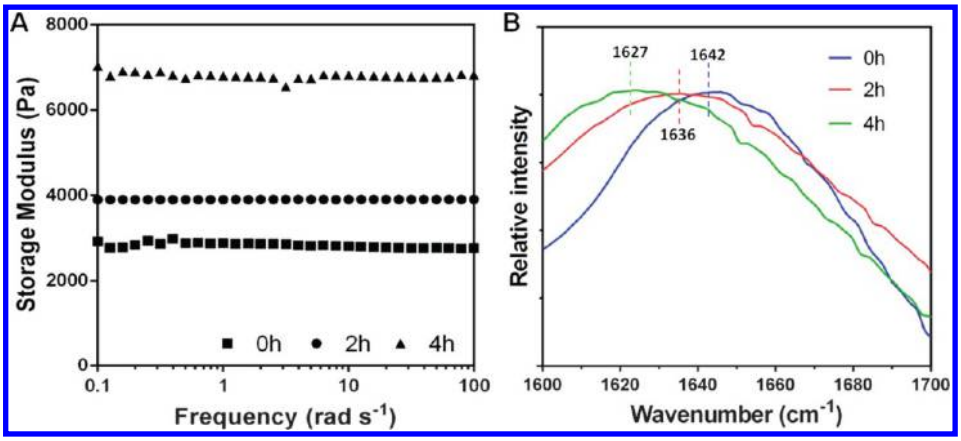

Figure 7. (A) Storage moduli (G') as a function of frequency and (B) FTIR absorbance spectra for the RS hydrogels. Freshly prepared 20% (w/v) RS solutions, without and with preincubation at 37 °C for either 2 or 4 h, were mixed with the photochemical cross-linking reagents and irradiated with white light to form hydrogels.

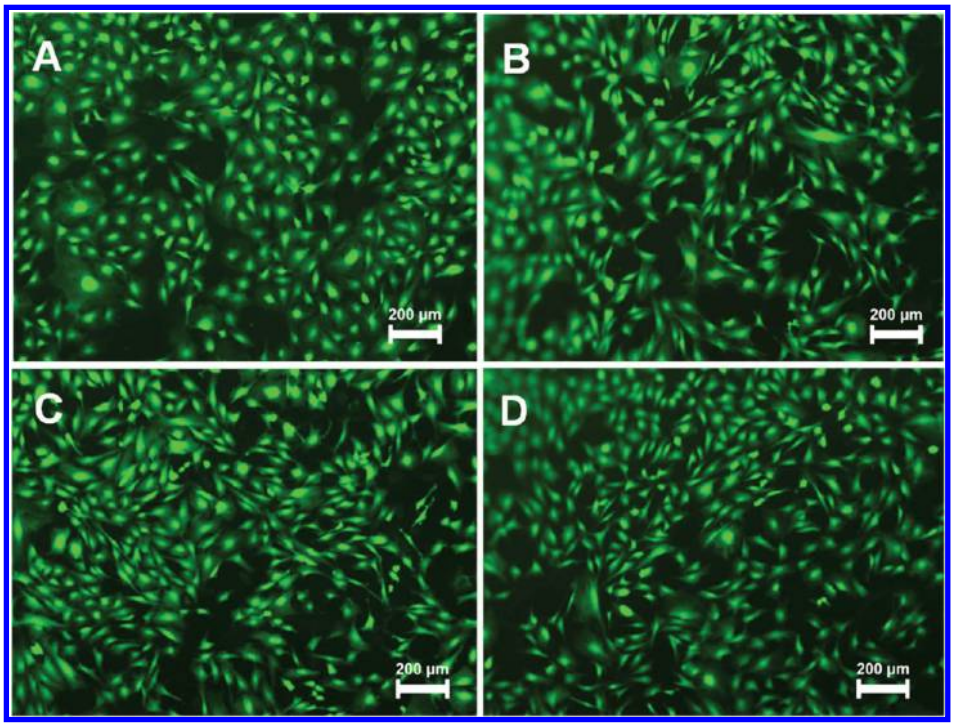

Figure 8. Live/Dead staining of cell viability for (A) the mouse preosteoblast MC3T3 cells seeded on TCP and (B) the photochemically cross-linked hydrogels without and with preincubation of the RS solution for (C) 2 or (D) 4 h. The mouse cells were incubated for 48 h, and stained with the LIVE/DEAD reagents. The living cells were fluorescent in green, and the dead cells in red.

To explore potential applications in cell culture, we evaluated in vitro cyto-compatibility of the photochemically cross-linked RS hydrogels using mouse preosteoblast cells (MC3T3-E1). Prior to cell seeding, the RS hydrogels were soaked and washed in PBS to remove excess photochemical reagents completely. The cells were then seeded on the surface of the hydrogels and the TCP plate, which served as a control. Live/Dead staining of the cells was performed at 48 h following inoculation and fluorescence images were then taken (Figure 8). It appeared that almost all the cells seeded on the TCP plate and the hydrogels were viable. Osteoblast attachments were also observed as the cells took on a stretched morphology. In addition, the RS hydrogels were appreciably stable as no observable difference existed before and after the cell culture. Taken together, these results indicated good cyto-compatibility of the photochemically cross-linked RS hydrogels. It would be interesting to examine whether these hydrogels are suitable for supporting growth of other cell lines, and to explore the outcome of tunable hydrogel mechanical property for tissue engineering applications in future studies.

CONCLUSIONS

In summary, we have for the first time biosynthesized a genetically engineered RS copolymer and demonstrated its self-assembly into diverse types of nanostructures in processes that are both temperature- and time-dependent (Figure 9). At 4 °C, RS self-assembled into micellar-like nanoparticles with a core of less soluble silk blocks and a hydrated corona composed of more soluble resilin blocks. At 37 °C, some micelles were aligned and assembled linearly into nanofibrils due to the

DOI: 10.1021/acsbiomaterials.7b00353
ACS Biomater. Sci. Eng. 2017, 3, 1576−1585

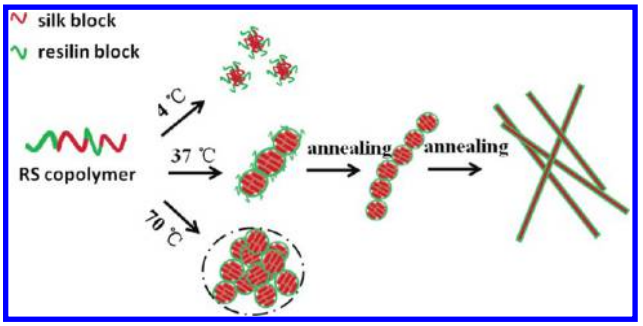

Figure 9. Proposed model for hierarchical assembly of RS.

increased hydrophobic interaction of silk blocks leading to the stacking of β-sheets. When the temperature was further increased to 70 °C, coacervates formed from the coalescence of the smaller micellar-like particles or nanofibrils. The proposed model for hierarchical assembly of the RS copolymer may need further investigations for precise understanding of the molecular events and mechanisms.

More importantly, the hierarchical assembly behavior of the RS copolymer has inspired attempts to fabricate complex, hierarchically structured materials. Of particular interest, the higher ordered nanofibers of RS upon incubation at the desirable body temperature enabled the formation of physically cross-linked hydrogel materials. In addition, preassembly of the RS copolymer along with chemical cross-linking have provided a novel strategy to modulate the resulting material properties. Therefore, the hierarchical assembly may provide intriguing opportunities to generate innovative dynamic materials for various applications. We anticipate that the newly developed RS may be potentially useful for controlled drug delivery and tissue engineering.

■ ASSOCIATED CONTENT

Supporting Information

The Supporting Information is available free of charge on the ACS Publications website at DOI: 10.1021/acsbiomaterials.7b00353.

Mass spectroscopy analysis of the purified protein polymers (Figure S1), hydrodynamic radius determination DLS plots (Figures S2 and S4), AFM images (Figure S3), test of formation of RS hydrogels in PBS (Figure S5), and full FTIR spectra of the photochemically cross-linked hydrogels (Figure S6) (PDF)

■ AUTHOR INFORMATION

Corresponding Author

*E-mail: xiaoxiaxia@sjtu.edu.cn.

ORCID

Xiao-Xia Xia: 0000-0001-8375-1616

Author Contributions

†S.-C.H. and Z.-G.Q. contributed equally to this work.

Notes

The authors declare no competing financial interest.

■ ACKNOWLEDGMENTS

Financial support was provided by the National Natural Science Foundation of China (31470216, 21674061, and 21406138). The authors also appreciate Instrumental Analysis Center of Shanghai Jiao Tong University for allowing us to use the AFM and SEM equipment.

■ REFERENCES

(1) Wegst, U. G.; Bai, H.; Saiz, E.; Tomsia, A. P.; Ritchie, R. O. Bioinspired structural materials. *Nat. Mater.* **2015**, *14*, 23−36.
(2) Gomes, S.; Leonor, I. B.; Mano, J. F.; Reis, R. L.; Kaplan, D. L. Natural and genetically engineered proteins for tissue engineering. *Prog. Polym. Sci.* **2012**, *37*, 1−17.
(3) Ebrahimi, D.; Tokareva, O.; Rim, N. G.; Wong, J. Y.; Kaplan, D. L.; Buehler, M. J. Silk-its mysteries, how it is made, and how it is used. *ACS Biomater. Sci. Eng.* **2015**, *1*, 864−876.
(4) Ding, D.; Guerette, P. A.; Hoon, S.; Kong, K. W.; Cornvik, T.; Nilsson, M.; Kumar, A.; Lescar, J.; Miserez, A. Biomimetic production of silk-like recombinant squid sucker ring teeth proteins. *Biomacromolecules* **2014**, *15*, 3278−3289.
(5) Xia, X. X.; Qian, Z. G.; Ki, C. S.; Park, Y. H.; Kaplan, D. L.; Lee, S. Y. Native-sized recombinant spider silk protein produced in metabolically engineered *Escherichia coli* results in a strong fiber. *Proc. Natl. Acad. Sci. U. S. A.* **2010**, *107*, 14059−14063.
(6) Girotti, A.; Orbanic, D.; Ibáñez-Fonseca, A.; Gonzalez-Obeso, C.; Rodríguez-Cabello, J. C. Recombinant technology in the development of materials and systems for soft-tissue repair. *Adv. Healthcare Mater.* **2015**, *4*, 2423−2455.
(7) Gustafson, J. A.; Ghandehari, H. Silk-elastinlike protein polymers for matrix-mediated cancer gene therapy. *Adv. Drug Delivery Rev.* **2010**, *62*, 1509−1523.
(8) Rombouts, W. H.; de Kort, D. W.; Pham, T. T.; van Mierlo, C. P.; Werten, M. W.; de Wolf, F. A.; van der Gucht, J. Reversible temperature-switching of hydrogel stiffness of coassembled, silk-collagen-like hydrogels. *Biomacromolecules* **2015**, *16*, 2506−2513.
(9) Liang, Y.; Li, L.; Scott, R. A.; Kiick, K. L. 50th anniversary perspective: polymeric biomaterials: diverse functions enabled by advances in macromolecular chemistry. *Macromolecules* **2017**, *50*, 483−502.
(10) Qian, Z. G.; Zhou, M. L.; Song, W. W.; Xia, X. X. Dual thermosensitive hydrogels assembled from the conserved C-terminal domain of spider dragline silk. *Biomacromolecules* **2015**, *16*, 3704−3711.
(11) Petitdemange, R.; Garanger, E.; Bataille, L.; Bathany, K.; Garbay, B.; Deming, T. J.; Lecommandoux, S. Selective tuning of elastin-like polypeptide properties via methionine oxidation. *Biomacromolecules* **2017**, *18*, 544−550.
(12) Lin, C. Y.; Liu, J. C. Modular protein domains: an engineering approach toward functional biomaterials. *Curr. Opin. Biotechnol.* **2016**, *40*, 56−63.
(13) Loo, Y.; Goktas, M.; Tekinay, A. B.; Guler, M. O.; Hauser, C. A.; Mitraki, A. Self-assembled proteins and peptides as scaffolds for tissue regeneration. *Adv. Healthcare Mater.* **2015**, *4*, 2557−2586.
(14) Aghaei-Ghareh-Bolagh, B.; Mithieux, S. M.; Weiss, A. S. Elastic proteins and elastomeric protein alloys. *Curr. Opin. Biotechnol.* **2016**, *39*, 56−60.
(15) Schacht, K.; Scheibel, T. Processing of recombinant spider silk proteins into tailor-made materials for biomaterials applications. *Curr. Opin. Biotechnol.* **2014**, *29*, 62−69.
(16) Chen, L.; Zhou, M. L.; Qian, Z. G.; Kaplan, D. L.; Xia, X. X. Fabrication of protein films from genetically engineered silk-elastin-like proteins by controlled cross-Linking. *ACS Biomater. Sci. Eng.* **2017**, *3*, 335−341.
(17) Li, L.; Kiick, K. L. Resilin-based materials for biomedical applications. *ACS Macro Lett.* **2013**, *2*, 635−640.
(18) Su, R. S.; Kim, Y.; Liu, J. C. Resilin: protein-based elastomeric biomaterials. *Acta Biomater.* **2014**, *10*, 1601−1611.
(19) Ardell, D. H.; Andersen, S. O. Tentative identification of a resilin gene in *Drosophila melanogaster*. *Insect Biochem. Mol. Biol.* **2001**, *31*, 965−970.
(20) Elvin, C. M.; Carr, A. G.; Huson, M. G.; Maxwell, J. M.; Pearson, R. D.; Vuocolo, T.; Liyou, N. E.; Wong, D. C.; Merritt, D. J.;

Dixon, N. E. Synthesis and properties of crosslinked recombinant pro-resilin. *Nature* **2005**, *437*, 999−1002.
(21) Lyons, R. E.; Wong, D. C.; Kim, M.; Lekieffre, N.; Huson, M. G.; Vuocolo, T.; Merritt, D. J.; Nairn, K. M.; Dudek, D. M.; Colgrave, M. L.; Elvin, C. M. Molecular and functional characterisation of resilin across three insect orders. *Insect Biochem. Mol. Biol.* **2011**, *41*, 881−890.
(22) Qin, G.; Lapidot, S.; Numata, K.; Hu, X.; Meirovitch, S.; Dekel, M.; Podoler, I.; Shoseyov, O.; Kaplan, D. L. Expression, cross-linking, and characterization of recombinant chitin binding resilin. *Biomacromolecules* **2009**, *10*, 3227−3234.
(23) Lyons, R. E.; Nairn, K. M.; Huson, M. G.; Kim, M.; Dumsday, G.; Elvin, C. M. Comparisons of recombinant resilin-like proteins: repetitive domains are sufficient to confer resilin-like properties. *Biomacromolecules* **2009**, *10*, 3009−3014.
(24) Tamburro, A. M.; Panariello, S.; Santopietro, V.; Bracalello, A.; Bochicchio, B.; Pepe, A. Molecular and supramolecular structural studies on significant repetitive sequences of resilin. *ChemBioChem* **2010**, *11*, 83−93.
(25) Dutta, N. K.; Truong, M. Y.; Mayavan, S.; Choudhury, N. R.; Elvin, C. M.; Kim, M.; Knott, R.; Nairn, K. M.; Hill, A. J. A genetically engineered protein responsive to multiple stimuli. *Angew. Chem., Int. Ed.* **2011**, *50*, 4428−4431.
(26) Balu, R.; Whittaker, J.; Dutta, N. K.; Elvin, C. M.; Choudhury, N. R. Multi-responsive biomaterials and nanobioconjugates from resilin-like protein polymers. *J. Mater. Chem. B* **2014**, *2*, 5936−5947.
(27) Truong, M. Y.; Dutta, N. K.; Choudhury, N. R.; Kim, M.; Elvin, C. M.; Hill, A. J.; Thierry, B.; Vasilev, K. A pH-responsive interface derived from resilin-mimetic protein Rec1-resilin. *Biomaterials* **2010**, *31*, 4434−4446.
(28) Qin, G.; Rivkin, A.; Lapidot, S.; Hu, X.; Preis, I.; Arinus, S. B.; Dgany, O.; Shoseyov, O.; Kaplan, D. L. Recombinant exon-encoded resilins for elastomeric biomaterials. *Biomaterials* **2011**, *32*, 9231−9243.
(29) Bracalello, A.; Santopietro, V.; Vassalli, M.; Marletta, G.; Del Gaudio, R.; Bochicchio, B.; Pepe, A. Design and production of a chimeric resilin-, elastin-, and collagen-like engineered polypeptide. *Biomacromolecules* **2011**, *12*, 2957−2965.
(30) Lv, S.; Dudek, D. M.; Cao, Y.; Balamurali, M. M.; Gosline, J.; Li, H. Designed biomaterials to mimic the mechanical properties of muscles. *Nature* **2010**, *465*, 69−73.
(31) Qin, G.; Hu, X.; Cebe, P.; Kaplan, D. L. Mechanism of resilin elasticity. *Nat. Commun.* **2012**, *3*, 1003.
(32) Whittaker, J. L.; Dutta, N. K.; Elvin, C.; Choudhury, N. R. Fabrication of highly elastic resilin/silk fibroin based hydrogel by rapid photo-crosslinking reaction. *J. Mater. Chem. B* **2015**, *3*, 6576−6579.
(33) Fernández-Colino, A.; Arias, F. J.; Alonso, M.; Rodríguez-Cabello, J. C. Self-organized ECM-mimetic model based on an amphiphilic multiblock silk-elastin-like corecombinamer with a concomitant dual physical gelation process. *Biomacromolecules* **2014**, *15*, 3781−3793.
(34) Xia, X. X.; Xu, Q.; Hu, X.; Qin, G.; Kaplan, D. L. Tunable self-assembly of genetically engineered silk-elastin-like protein polymers. *Biomacromolecules* **2011**, *12*, 3844−3850.
(35) Zhou, M. L.; Qian, Z. G.; Chen, L.; Kaplan, D. L.; Xia, X. X. Rationally designed redox-sensitive protein hydrogels with tunable mechanical properties. *Biomacromolecules* **2016**, *17*, 3508−3515.
(36) Zeng, L.; Jiang, L.; Teng, W.; Cappello, J.; Zohar, Y.; Wu, X. Engineering aqueous fiber assembly into silk-elastin-like protein polymers. *Macromol. Rapid Commun.* **2014**, *35*, 1273−1279.
(37) Beun, L. H.; Storm, I. M.; Werten, M. W.; de Wolf, F. A.; Cohen Stuart, M. A.; de Vries, R. From micelles to fibers: balancing self-assembling and random coiling domains in pH-responsive silk-collagen-like protein-based polymers. *Biomacromolecules* **2014**, *15*, 3349−3357.
(38) Elvin, C. M.; Brownlee, A. G.; Huson, M. G.; Tebb, T. A.; Kim, M.; Lyons, R. E.; Vuocolo, T.; Liyou, N. E.; Hughes, T. C.; Ramshaw, J. A.; Werkmeister, J. A. The development of photochemically crosslinked native fibrinogen as a rapidly formed and mechanically strong surgical tissue sealant. *Biomaterials* **2009**, *30*, 2059−2065.
(39) Elvin, C. M.; Vuocolo, T.; Brownlee, A. G.; Sando, L.; Huson, M. G.; Liyou, N. E.; Stockwell, P. R.; Lyons, R. E.; Kim, M.; Edwards, G. A.; Johnson, G.; McFarland, G. A.; Ramshaw, J. A.; Werkmeister, J. A. A highly elastic tissue sealant based on photopolymerised gelatin. *Biomaterials* **2010**, *31*, 8323−8331.
(40) Jeon, E. Y.; Hwang, B. H.; Yang, Y. J.; Kim, B. J.; Choi, B. H.; Jung, G. Y.; Cha, H. J. Rapidly light-activated surgical protein glue inspired by mussel adhesion and insect structural crosslinking. *Biomaterials* **2015**, *67*, 11−19.
(41) Bjork, J. W.; Johnson, S. L.; Tranquillo, R. T. Ruthenium-catalyzed photo cross-linking of fibrin-based engineered tissue. *Biomaterials* **2011**, *32*, 2479−2488.
(42) Hu, X.; Wang, X.; Rnjak, J.; Weiss, A. S.; Kaplan, D. L. Biomaterials derived from silk-tropoelastin protein systems. *Biomaterials* **2010**, *31*, 8121−8131.

DOI: 10.1021/acsbiomaterials.7b00353
ACS Biomater. Sci. Eng. 2017, 3, 1576−1585